

# TextMesh4D: Text-to-4D Mesh Generation via Jacobian Deformation Field

Sisi Dai<sup>1</sup> Xinxin Su<sup>1</sup> Ruizhen Hu<sup>3</sup> Kai Xu<sup>1,2</sup>

<sup>1</sup>National University of Defense Technology

<sup>2</sup>Institute of AI for Industries (IAII), Chinese Academy of Sciences (CAS) <sup>3</sup>Shenzhen University

## Abstract

*Dynamic 3D (4D) content generation, particularly text-to-4D, remains a challenging and under-explored problem due to its inherent spatiotemporal complexity. Existing text-to-4D methods typically avoid direct mesh generation due to inherent topological constraints, favoring alternative representations like NeRFs or 3DGS. However, these non-mesh approaches, suffer from insufficient geometric fidelity, temporal artifacts, and limited compatibility with modern computer graphics (CG) pipelines. In contrast, directly generating dynamic meshes faces two key challenges: i) deformation inflexibility, as traditional vertex-based optimization is constrained by meshes' explicitly encoded topology, and ii) semantic inconsistency, arising from stochastic noise in distilled priors.*

*In this paper, we introduce TextMesh4D, a pioneering framework for text-to-4D mesh generation that directly addresses these challenges. TextMesh4D features two core innovations: 1) the Jacobian Deformation Field (JDF), which shifts the deformation unit from vertices to faces, using per-face Jacobians to model flexible transformations free from topological constraints. 2) the Local-Global Semantic Regularizer (LGSR), which leverages the mesh's innate geometric properties to enforce semantic coherence both locally and globally across frames. Extensive experiments demonstrate that TextMesh4D achieves state-of-the-art performance in temporal consistency, structural fidelity, and visual realism, while requiring only a single 24GB GPU. Our work establishes a new benchmark for efficient and high-quality text-to-4D mesh generation. The code will be released to facilitate future research.*

## 1. Introduction

3D content generation has garnered significant attention with the popularity of various applications such as virtual reality, augmented reality, gaming, robotics simulation, etc. Recent advances in text-to-image/video diffusion models [6, 18, 45, 50, 52, 54, 59], along with prior distillation techniques such as Score Distillation Sampling (SDS) [38],

have substantially advanced zero-shot text-to-3D, overcoming the long-standing data-sparsity bottleneck. However, extending these advances to dynamic 3D (text-to-4D) remains largely unexplored due to the increased spatiotemporal complexity compared to static 3D generation.

Meshes retain significant advantages and priorities in modern computer graphics (CG) pipelines. However, their topology and connectivity restrict their ability to accommodate complex motions. Consequently, existing text-to-4D approaches circumvent direct mesh generation, instead adopting topologically flexible alternatives like Neural Radiance Fields (NeRFs) or 3D Gaussian Splatting (3DGS). While effective for appearance-priority synthesis, these methods face two key limitations: (i) Insufficient geometric fidelity. Such primitive-based representations frequently introduce floating artifacts and temporal flicker, which undermine both realism and temporal coherence; (ii) Usability restriction. Such outputs are incompatible with standard CG workflows and require lossy mesh conversion. Moreover, meshes converted from these methods suffer from inconsistent vertex connectivity.

A text-to-4D mesh solution is promising to address these limitations. However, two key challenges stand in the way: (i) **Deformation inflexibility**. Meshes explicitly encode geometry via vertices and topology through connectivity. While existing methods primarily optimize vertex displacements (directly or indirectly), the topology inherently restricts the vertex's freedom due to constraints from its neighbors, thereby causing inflexible deformation and limited motion expression. (ii) **Semantic inconsistency**. Mainstream text-to-4D methods distill prior knowledge from text-to-video (T2V) models for motion guidance. However, the stochastic nature of such priors leads to time-varying semantic inconsistency that manifests as both local disruptions and global identity drifts.

To address these challenges, our two key insights are: (i) **From vertices to faces**. We shift the deformation unit from vertices to faces. This allows each face to escape vertex constraints and express its transformation independently, naturally enhancing deformation flexibility. (ii) **Beyond distilled priors**. While distilled T2V priors are inherently stochastic,

leading to semantic inconsistency, we leverage the mesh’s geometric and topological properties to actively suppress the overly-stochastic motion noise from the prior.

To this end, we propose *TextMesh4D*, a novel framework incorporating two innovations built upon such insights: **1) Jacobian Deformation Field (JDF)**. This proposed field adopts per-face Jacobian matrices to model flexible deformations, freeing deformations from topological constraints. The Jacobians are then exploited to reconstruct the surface through Poisson integration, ensuring smoothness even under high-variance gradients, thereby achieving continuous and natural motion generation. **2) Local-Global Semantic Regularizer (LGSR)**. To ensure temporally consistent semantic motion, we introduce a Local-Global Semantic Regularizer that operates at the geometric level, both locally and globally. Specifically, the local part utilizes the mesh’s topological connectivity to stabilize local rigidity and suppress overly stochastic local noise. The global part preserves global semantic identity, thus enforcing frame-wise semantic coherence.

Our main contributions are summarized as follows:

- We introduce *TextMesh4D*, the pioneering framework for text-to-4D mesh generation.
- We propose the Jacobian Deformation Field (JDF), releasing deformations from topological constraints to unlock mesh flexibility and achieve continuous motion.
- We introduce the Local-Global Semantic Regularizer (LGSR), operating at the geometric level to preserve both local and global semantic coherence.
- Extensive experiments demonstrate state-of-the-art text-to-4D results, with improved temporal consistency, structural preservation, and visual fidelity, while maintaining low memory cost on a single 24GB GPU.

## 2. Related Work

**Text-to-Image/Video Generation.** In recent years, diffusion models have achieved significant advancements in image and video generation, including text-to-image (T2I) models [42, 45, 46], as well as text-to-video (T2V) models [1, 10, 59]. These models are trained on large-scale open-domain datasets, typically including LAION-5B [47], WebVid-10M [5], and HD-VG-130M [61]. Recent advancements in text-image-to-video generation (TI2V) have incorporated image-based semantic conditions into T2V models [13, 16, 62]. The latest model *DynamiCrafter* [64] employs a learnable image encoding network and dual cross-attention layers to effectively integrate text and image information, achieving impressive open-domain TI2V generation. Our work distills the generative power of video diffusion models for motion generation, with the belief that our method will evolve accordingly with the continued advancement of video generation technology.

**Text-to-3D Generation.** Early methods [11, 23, 31] for text-to-3D generation require paired data of 3D data and corresponding textual descriptions, which limits their generality to unseen object categories. Benefiting from large pre-trained text-to-image models and differentiable rendering techniques, breakthroughs [19, 24, 27, 36] in text-to-3D content generation have been achieved. Recently, the technique SDS (Score Distillation Sampling) has been introduced in the pioneering work *DreamFusion* [38], enabling 3D generation by distilling guidance from pre-trained T2I diffusion models. There are a lot of follow-up works to improve *DreamFusion*. Some focus on 3D representation [12, 29]: *Magic3D* [29] proposes a coarse-to-fine pipeline to generate the fine-grained mesh; *TextMesh* [57] extends the geometry representation from NeRF to an SDF framework, enhancing detailed mesh extraction and photo-realistic rendering; *DreamGaussian* [55] proposes to adopt 3D Gaussian Splatting to increase efficiency. Some works focus on improving SDS: *SJC* [58] proposes a variant of SDS, while *VSD* are proposed in *ProlificDreamer* [63]; *DreamTime* [20] improves the generation quality by modifying the timestep sampling strategy. Others focus on inducing 3D priors into the guidance source, which effectively alleviates the Janus problem. Additional 3D priors are introduced in shape [8, 14, 21, 34, 37, 66], providing geometric initial values for optimizing NeRF. *MV-Dream* [49] proposes to fine-tune the diffusion model to generate multi-view images, thereby explicitly embedding 3D information into a 2D diffusion model. Moreover, works on image-based generation [33, 39, 56] and text-based editing [17, 28, 48, 69] are also boosted by utilizing these capabilities. Our first static stage performs text-to-3D generation with our Jacobian-based representation.

**Text-to-4D Generation.** The pioneering effort, *MAV3D* [51], combines a T2V diffusion model with dynamic NeRFs and *HexPlane* [7] to optimize both scene appearance and motion consistency. Building on this foundation, *4D-fy* [3] employs a hybrid SDS approach that integrates T2I, 3D-aware T2I, and T2V diffusion models to achieve high-fidelity 4D generation. *Align Your Gaussians* (AYG) [30] employs dynamic 3D Gaussian splatting to reduce optimization time while enhancing temporal consistency. *TC4D* [4] introduces trajectory conditioning to maintain coherence between global and local motion. Although these methods have demonstrated effectiveness, they often rely heavily on NeRF and video models, leading to substantial computational costs. *Comp4D* [65] employs a Large Language Model (LLM) to segment input prompts into distinct entities, generating 4D objects independently and then combining them based on trajectory data provided by the LLM. Our work pioneers text-to-4D generation using a mesh representation.

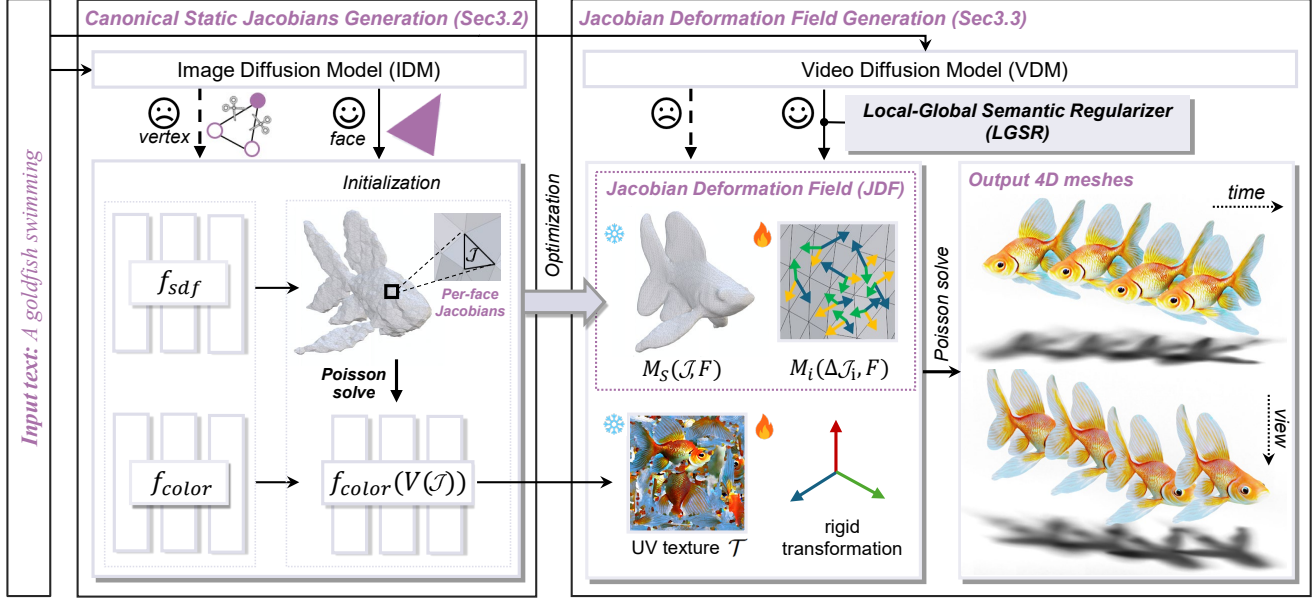


Figure 1. Overview of our TextMesh4D. Given a text prompt, we aim to generate 4D mesh in line with the prompt. To achieve this, we propose Jacobian Deformation Field (JDF) and local-global semantic regularizer (LGSR). In the first static stage, we generate a high-quality static 3D with canonical static Jacobians, by guidance from image diffusion priors. In the second dynamic stage, we generate the dynamic motion with Jacobians’ deformation and rigid transformation, with tailored local-global semantic regularizer.

### 3. Method

Our goal is to generate 4D meshes from text prompts, using distilled priors from pre-trained diffusion models in a zero-shot manner. The input is a given text prompt describing both the desired object and motion. The output is a sequence of textured 3D meshes, formulated as  $\mathcal{M} = \{\mathcal{M}_i = (\mathcal{V}_i, \mathcal{F}, \mathcal{T})\}_{i=1}^L$ , where  $\mathcal{V}_i$  denotes the vertices of the  $i$ -th mesh, which vary across sequence to capture the motion.  $\mathcal{F}$  represents the faces,  $\mathcal{T}$  indicates the UV texture map, and  $L$  is the length of the sequence.

We first introduce our proposed Jacobian Deformation Field (Sec. 3.1) and then explain how the total 4D parameters are optimized, covering the static stage (Sec. 3.2) and the dynamic stage (Sec. 3.3).

#### 3.1. Jacobian Deformation Field

The total 4D mesh parameters consist of decomposed parts: 1) static parameters for a textured 3D mesh,  $\mathcal{M}_s = \{\mathcal{V}_s, \mathcal{F}, \mathcal{T}\}$ ; 2) a sequence of dynamic parameters  $\Theta = \{\theta_i = \{\Delta \mathcal{V}_i, \mathcal{R}_i\}\}_{i=1}^L$ , comprising the desired motion including both deformation  $\Delta \mathcal{V}_i$ , and rigid transformation  $\mathcal{R}_i$  with global translation and rotation, where  $L$  is the length of the sequence. Therefore, the output mesh sequence is  $\mathcal{M} = \{\mathcal{M}_i = (\mathcal{R}_i(\mathcal{V}_s + \Delta \mathcal{V}_i), \mathcal{F}, \mathcal{T})\}_{i=1}^L$ .

To effectively model the deformation  $\Delta \mathcal{V}_i$ , we shift our modeling unit from vertices to faces. Specifically, we propose Jacobian Deformation Field (JDF), which is defined

by per-face Jacobian matrices. The JDF is then composed of canonical static Jacobians and dynamic deformations for time-varying motion.

**Per-face Jacobians.** At each triangle  $f_j$  of mesh  $\mathcal{M}$ , the Jacobian  $J_j \in \mathbb{R}^{3 \times 3}$  is a linear transformation from the triangle’s tangent space to vertex space  $\mathcal{V} \in \mathbb{R}^3$ . Defining the deformation as vertex displacement  $\Delta \mathcal{V}$  via  $\Phi$ , a linear operator  $\nabla_j$  is yielded to associate each  $\Phi$  with corresponding Jacobian matrix  $\nabla_j(\Phi)$ . The Jacobian  $\nabla_j(\Phi)$  restricts  $\Phi$  within each triangle  $f_j$ , inherently providing low-frequency, smooth signals for deformation as vertex positions.

Given a target assignment of Jacobian  $J_j$ , a deformation map  $\Phi^*$  can be solved following the Poisson equation in a least-squares sense:

$$\Phi^* = \min_{\Phi} \sum_{f_j \in \mathcal{F}} |f_j| \|\nabla_j(\Phi) - J_j\|_2^2,$$

where  $|f_j|$  is the area of triangle  $f_j$ . With deformation map  $\Phi^*$  embedding the entire mesh,  $\Phi$  can be optimized indirectly by optimizing the Jacobian matrices  $\mathcal{J} = \{J_j\}$  for each face. We then leverage a differentiable Poisson solver layer [2] for our optimization.

**Jacobian Deformation Field.** To achieve high-quality generation, rather than basing on direct vertex positions, we build the parametrization upon Jacobians  $\mathcal{J} = \{J_j\}$

at each triangle as the mesh representation, thereby facilitating smooth, continuous, and globally consistent deformations. Thus, as illustrated in Fig. 1, our method consists of two stages: 1) *Canonical Static Jacobians Generation*. First, we optimize for a high-quality static 3D model  $\mathcal{M}_s$ , the parameters are substituted by Jacobians as  $\mathcal{M}_s = \{\mathcal{V}_0 + \Delta\mathcal{V}, \mathcal{F}, \mathcal{T}\} = \{\mathcal{V}_0 + \mathcal{J}, \mathcal{F}, \mathcal{T}\}$ , where  $\mathcal{V}_0$  and  $\mathcal{F}$  are initialized parameters by an SDF network; 2) *Jacobian Deformation Field Optimization*. With the static parameters fixed, dynamic parameters  $\Theta = \{\theta_i = \{\Delta\mathcal{V}_i, \mathcal{R}_i\}\}_{i=1}^L$  are also represented by delta Jacobians as  $\Theta = \{\theta_i = \{\Delta\mathcal{J}_i, \mathcal{R}_i\}\}_{i=1}^L$ , which are then optimized.

### 3.2. Canonical Static Jacobians Generation

**Initialization.** Recall that at this stage, our objective is to generate a high-quality, textured 3D mesh solely from an input text prompt. We observe that learning large topological changes via direct mesh initialization (e.g., spot) is challenging for arbitrary inputs and often results in unsatisfactory mesh quality. To this end, we adopt NeuS [60] for mesh initialization. NeuS [60] is a volume rendering method that integrates the advantages of signed distance functions (SDF) and Neural Radiance Fields (NeRF) [35], better for extracting a 3D geometry and obtaining a mesh as the initialization for further high-quality generation. We denote the NeuS  $\mathcal{N} = \{f_{sdf}, f_{color}\}$ , both  $f_{sdf}$  and  $f_{color}$  are networks implemented using MLPs, outputting the SDF and color at point  $p$ , respectively. The NeuS is then optimized with supervision provided by combined diffusion priors under input text conditioning. After optimization, we extract the surface at the zero-level set of SDF as the initial mesh  $\mathcal{M}_0$  using the marching cubes algorithm [32].

**Optimization via Jacobians.** The extracted mesh  $\mathcal{M}_0$  consists of a set of vertices  $\mathcal{V}_0 \in \mathbb{R}^{N \times 3}$ , faces  $\mathcal{F} \in \mathbb{R}^{M \times 3}$ , which is converted to the representation of differentiable Jacobians,  $\{\mathcal{V}_0 + \mathcal{J}, \mathcal{F}\}$ , where the Jacobians are initialized as identity matrices for optimization. We inherit the weights of the color network from the initialization phase and continue to refine them. However, unlike the initialization phase, which utilizes random sampling points, the sampling in this phase is focused on regions near the initialized surface. Thus, we denote the color network at this phase as  $f_{color}(\mathcal{J})$ . This concentrated sampling strategy allows for a more precise refinement of the color generation.

To achieve high-quality generation, we employ combined diffusion priors from both 3D-aware and 2D-image diffusion models, following [3, 68]. The 3D-aware diffusion model, e.g., MVDream [49], is trained with multi-view embeddings along with camera parameters, providing a 3D prior and alleviating the Janus problem. As for the 2D-image diffusion priors, we incorporate an additional loss term based on the variational score distillation (VSD) for appearance improvement. Combined SDS with them lever-

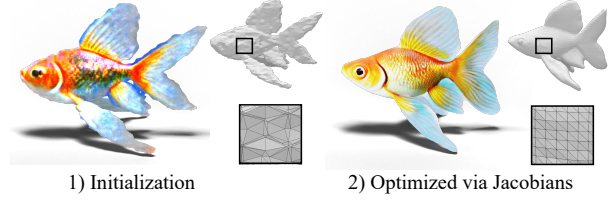


Figure 2. Comparison including geometry and texture between initialization and subsequent jacobian-based generation.

ages the complementary strengths of 3D-aware and 2D-image diffusion models, resulting in a better generation for our static object:

$$\mathcal{L}_{\text{static}} = \lambda_{3D}\mathcal{L}_{\text{SDS-3D}} + \lambda_{2D}\mathcal{L}_{\text{SDS-2D}}, \quad (1)$$

The loss weights  $\{\lambda_{3D}, \lambda_{2D}\}$  are carefully tuned for better generation. They are set to  $\{0.7, 0.3\}$  during the initialization stage and adjusted to  $\{0.5, 0.5\}$  subsequently. Please refer to the supplementary material for loss details.

To sum up, during the initialization stage, we optimize the networks  $\{f_{sdf}, f_{color}\}$ . After initialization, with the initialized  $\mathcal{M}_0$ , parameters that further need to be optimized are  $\{\mathcal{J}, f_{color}(\mathcal{J})\}$ . Finally, the UV-space texture map  $\mathcal{T}$  is extracted from  $f_{color}(\mathcal{J})$  for the subsequent motion generation. Fig. 2 illustrates the evolution from the initialization phase to the final generation at this stage.

### 3.3. Jacobian Deformation Field Optimization

With the static parameters fixed, we then optimize the dynamic parameters  $\Theta = \{\theta_i = \{\Delta\mathcal{J}_i, \mathcal{R}_i\}\}_{i=1}^L$  to produce the vivid 3D motion. Note that a differentiable renderer is required to project the textured mesh sequence with  $\mathcal{T}$  to the image space, thus enabling gradient steps during optimization at this stage. We implement the renderer based on NVdiffrast [26] as follows:

$$R(\cdot|C) := \mathcal{M}_i^{\theta_i, \mathcal{M}_s} \mapsto I^{\mathcal{M}_i} \in \mathbb{R}^{H \times W}, \quad (2)$$

where  $H$  and  $W$  denote the height and width of the rendered image, with  $C$  representing the camera extrinsics.

**Objective Function.** The overall objective function at this stage is:

$$\mathcal{L}_{\text{dynamic}} = \mathcal{L}_{\text{VDS}} + \mathcal{L}_{\text{LGSr}} + \mathcal{L}_{\text{others}} \quad (3)$$

We distill video diffusion priors to provide semantic motion guidance by video score distillation sampling (VDS). This procedure queries a video diffusion model [1], to see how a rendered video from our representation aligns with the input prompt, through the noise sampling of video diffusion process. The gradients are then backpropagated to the dynamic parameters. Please refer to the supplementary for the corresponding loss  $\mathcal{L}_{\text{VDS}}$  computation.

However, the stochastic nature of VDS introduces distortions and unstable convergence into the optimization. To address this issue, we design the tailored regularization term  $\mathcal{L}_{\text{LGSR}}$ , with a synergy of local and global semantic regularity at geometric level,  $\mathcal{L}_{\text{L-SR}} + \mathcal{L}_{\text{G-SR}}$ , for Jacobians’ robust optimization under guidance from video score distillation sampling.

$\mathcal{L}_{\text{G-SR}}$  is a global semantic regularization term on the optimized Jacobians to prevent the divergence too far from the static object’s geometry during dynamic optimization, inspired by [15]. This term ensures the global geometry is preserved while still allowing for flexible deformations that capture motion semantics. Specifically, the term penalizes the difference between the dynamic Jacobians  $\{J + \Delta J_i\}$  and the static identity with a weight:

$$\mathcal{L}_{\text{G-SR}} = \sum_{i=0}^{\ell-1} \sum_{j=0}^{|f|-1} e^{\|\hat{J}_j - I\|} \|\hat{J}_j - I\|_2, \quad (4)$$

We then further employ As-Rigid-As-Possible (ARAP) energy [22] as the rigidity regularization term  $\mathcal{L}_{\text{L-SR}}$ :

$$\mathcal{L}_{\text{L-SR}} = \sum_{i=0}^{\ell-1} \sum_{j=0}^{n-1} \sum_{k \in \mathcal{N}_{v_j}} w_{j,k} \|(v_j^i - v_k^i) - R_j(v_j^s - v_k^s)\|^2, \quad (5)$$

where  $\mathcal{N}_{v_j}$  represents the one-ring neighborhoods of vertex  $v_j$ .  $w_{j,k} = (\cot \alpha_{jk} + \cot \beta_{jk}) / 2$ , measuring the impact of  $v_k$  on  $v_j$ .  $\alpha_{jk}$  and  $\beta_{jk}$  are the angles on the faces adjacent to the edge  $(v_j, v_k)$ , which are opposite the edge itself.  $R_j$  represents the optimal rotation estimated by Singular Value Decomposition (SVD) [22]. This term encourages the generation to maintain local rigidity during the deformation.

The Local-Global Semantic Regularizer (LGSR) both preserves local rigidity and maintains global semantic coherence, thereby improving the temporal semantic consistency of the motion, as demonstrated in our ablation studies. We leave additional details of the other regularizers, e.g., smoothness term and Jacobian’s dof regularization, in the supplementary.

## 4. Experiments

To evaluate the effectiveness of TextMesh4D, we conduct a comprehensive comparison with state-of-the-art text-to-4D methods across geometric fidelity, appearance quality, motion vividness, semantic consistency, and overall performance. In addition, we benchmark TextMesh4D against representative image-, video-, and 3D-to-4D methods, including both zero-shot and data-driven paradigms, to further assess its capability in 4D content generation. Experimental results demonstrate that TextMesh4D achieves superior performance.

---

### Algorithm 1 TextMesh4D

---

**Require:**

<i>text</i>	▷ input text prompt
$\mathcal{M} = \{\mathcal{M}_s, \Theta\}$	▷ 4D representation
$\mathcal{M}_s = \{\mathcal{V}_0 + \mathcal{J}, \mathcal{F}, \mathcal{T}\}$	▷ static part
$\Theta = \{\theta_i = \{\Delta \mathcal{J}_i, \mathcal{R}_i\}\}_{i=1}^L$	▷ dynamic part
$N_{\text{stage-1}}, N_{\text{stage-2}}$	▷ iterations for each stage
$\mathcal{L}_{\text{SDS-2D}}, \mathcal{L}_{\text{SDS-3D}}, \mathcal{L}_{\text{VDS}}$	▷ SDS losses
$\mathcal{L}_{\text{G-SR}}, \mathcal{L}_{\text{L-SR}}, \mathcal{L}_{\text{smooth}}, \mathcal{L}_{\text{dof}}$	▷ regularization terms

- 1: // **Stage 1**
  - 2: Initialize  $\mathcal{M}_0(\mathcal{V}_0, \mathcal{F})$  by NeuS
  - 3: Parameterize  $\mathcal{M}_s = \{\mathcal{V}_0 + \mathcal{J}, \mathcal{F}, \mathcal{T}\}$  by Jacobians
  - 4: **for** iter  $\in N_{\text{stage-1}}$  **do** ▷ static update
  - 5:     **grad** =  $\nabla_{\mathcal{J}, \mathcal{T}} \mathcal{L}_{\text{SDS-2D}} + \nabla_{\mathcal{J}, \mathcal{T}} \mathcal{L}_{\text{SDS-3D}} + \lambda_0 \nabla_{\mathcal{J}, \mathcal{T}} \mathcal{L}_{\text{dof}}$
  - 6:     UPDATE (**grad**)
  - 7: **end for**
  - 8: // **Stage 2**
  - 9: Parameterize  $\Theta = \{\theta_i = \{\Delta \mathcal{J}_i, \mathcal{R}_i\}\}_{i=1}^L$  by delta Jacobians
  - 10: **for** iter  $\in N_{\text{stage-2}}$  **do** ▷ dynamic update
  - 11:     **grad** =  $\nabla_{\Theta} \mathcal{L}_{\text{VDS}} + \lambda_1 \nabla_{\Theta} \mathcal{L}_{\text{G-SR}} + \lambda_2 \nabla_{\Theta} \mathcal{L}_{\text{L-SR}} + \lambda_3 \nabla_{\Theta} \mathcal{L}_{\text{smooth}} + \lambda_4 \nabla_{\Theta} \mathcal{L}_{\text{dof}}$
  - 12:     UPDATE (**grad**)
  - 13: **end for**
- 

### 4.1. Implementation Details

We summarize our TextMesh4D in Algorithm 1. The  $\lambda_1$ ,  $\lambda_2$ ,  $\lambda_3$ , and  $\lambda_4$  in the loss function are respectively set as 0.1, 0.0001, 0.1, and 0.1. We optimize TextMesh4D using Adam [25] with a learning rate of 0.01, on an NVIDIA RTX 6000 GPU, with an approximate memory consumption of 24GB. The total optimization time for the static stage and the dynamic stage is approximately 1.5 hours. See Supplementary Material for additional details.

### 4.2. Experimental Setup

**Evaluation Baselines.** Evaluation baselines are divided into two main categories: 1) Zero-shot Methods. Our primary comparison is against SOTA zero-shot methods that distill diffusion priors. These are further divided into: i) NeRF-based methods, including 4D-fy, Dream-in-4D (text/image-to-4D), and TC4D; ii) 3DGS-based methods, including AYG and DG4D (image-to-4D). 2) Data-driven Methods. To ensure the evaluation is comprehensive and provide a broader context, we also include comparisons against data-driven SOTA approaches (which use different paradigms or inputs), including Puppeteer (3D-to-4D), STAG4D (text/video-to-4D), and L4GM (video-to-4D).

The evaluation prompts are the union of prompt sets from the baseline papers. All baseline results were generated using their official GitHub repositories and default configurations. For methods with unavailable code (e.g.,

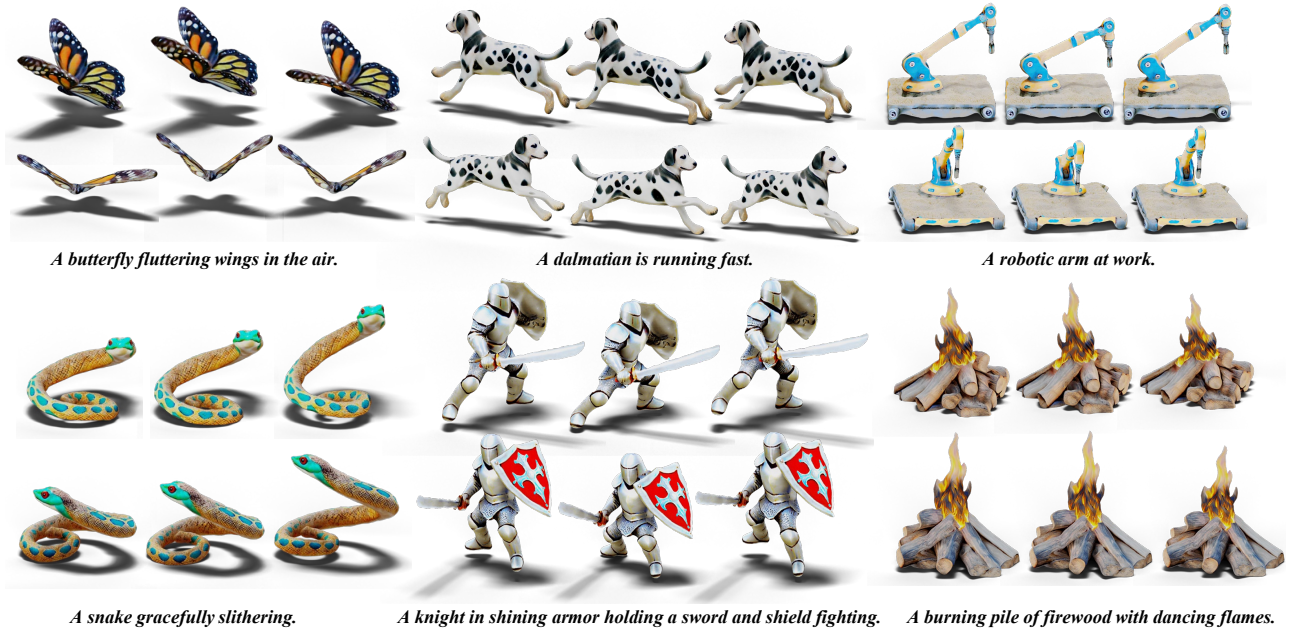


Figure 3. Diverse 4D generation results by TextMesh4D.

AYG), we use their official project page videos for qualitative comparison. Note that we exclude CT4D [9] from our quantitative comparisons, as its official implementation and results were not publicly available at the time of our experiments. However, we provide a qualitative visual comparison in the supplementary material by using images directly from the paper.

**Evaluation metrics.** Quantitatively evaluating text-to-4D generation remains challenging due to the lack of ground-truth data. To enable a comprehensive and reliable quantitative evaluation, we adopt evaluation metrics comprising CLIP score, GPT-4V selection, and perceptual user studies, collectively covering multiple quality dimensions.

### 4.3. Qualitative Evaluations

**Diverse results.** In Fig.3, we present a diverse collection of our generated 4D results, which demonstrates our method’s capability in generating diverse and complex motions. Our TextMesh4D successfully handled various rigid or non-rigid deformations, including articulated animal motions (butterfly) or human motions (knight), robotic motions (robotic arm), soft-body deformations (snake), and fluid-like behaviors (flame).

**Comparison results.** Our qualitative comparison focuses on the underlying geometry representation of 4D content, as this is central to our method’s contribution. To reveal the geometric fidelity of different 4D representations, we select representative baselines with publicly available code, making their underlying geometry accessible. We adopt 4D-

fy [3], a publicly available NeRF-based method for text-to-4D generation, and DreamGaussian4D [43], a 3DGS-based method for image-to-4D generation. For fairness, we input text prompts into a SOTA text-to-image model to generate high-quality images, which then serve as inputs for DreamGaussian4D. Together with our mesh-based approach, this selection ensures our qualitative comparison covers the mainstream geometry representations: NeRF, 3DGS, and mesh.

As shown in Fig.4 (overall comparison), together with Fig.5 (geometric preservation) and Fig. 6 (appearance and motion vividness), we present a comprehensive comparison of 4D generation results. Our method significantly outperforms the baselines across all evaluation dimensions. The implicit representations used by the baselines, specifically NeRF in 4D-fy and 3D Gaussian Splatting (3DGS) in DreamGaussian4D, cause most of the generated motion to manifest as floating artifacts in the geometric space, making the results visually ambiguous and difficult to interpret. Moreover, because these methods do not model global transformations, the generated motion remains confined to local object regions, which further limits their expressive capability. In contrast, our method employs a mesh representation that integrates both local deformations and global transformations, enabling effective spatial movement solely conditioned on input text.

### 4.4. Quantitative Evaluations

**CLIP Score.** Following common practice, we compute the CLIP score [40] to measure the similarity between input text prompts and the corresponding generated results,

Table 1. Quantitative comparisons with 4d-fy and DreamGaussian4D. The methods are evaluated in terms of CLIP Score, GPT-4V selection, and metrics of the user study.

Method	Geometry	Condition	CLIP↑	GPT-4V Selection (%)					User Studies					GPU requirement
				AQ↑	SQ↑	MQ↑	TA↑	Overall↑	AQ↑	SQ↑	MQ↑	TA↑	Overall↑	
4D-fy [3]	NeRF	Text	31.03	5.68	8.02	3.57	8.42	5.36	3.1	2.9	1.5	2.6	2.4	1 * A100 80GB
Dream-in-4D [68]	NeRF	Text/Image	31.67	4.22	7.71	6.19	10.36	6.03	2.3	2.9	2.6	3.2	2.7	1 * A100 80GB
TC4D [4]	NeRF	Text	31.83	4.95	7.40	3.81	6.79	5.58	2.7	2.9	1.6	2.1	2.5	1 * A100 80GB
AYG [30]	Gaussian primitive	Text	30.14	6.23	8.24	9.05	11.65	8.04	3.4	3.1	3.8	3.6	3.6	128 * A100 80GB
DG4D [43]	Gaussian primitive	Text	28.70	2.20	2.92	3.33	5.18	2.90	1.2	1.1	1.4	1.6	1.3	1 * A100 80GB
STAG4D [67]	Gaussian primitive	Text/Video	31.93	5.13	6.91	4.53	11.33	6.92	2.8	2.6	1.9	3.5	3.1	1 * 3090 24GB
L4GM [44]	Gaussian primitive	Video	N/A	4.48	9.11	8.29	N/A	7.69	2.9	3.4	2.7	N/A	3.2	128 * A100 80GB
3-to-4D [41]	NeRF	Text+3D	29.62	4.22	7.44	7.39	7.81	6.03	2.3	2.8	3.1	2.4	2.7	1 * A100 80GB
Puppeteer [53]	Mesh	3D	N/A	6.05	10.10	8.10	N/A	8.26	3.3	3.8	3.4	N/A	3.7	8 * A100 80GB
<b>Ours</b>	<b>Mesh</b>	<b>Text</b>	<b>32.32</b>	<b>56.82</b>	<b>32.16</b>	<b>45.70</b>	<b>38.45</b>	<b>43.19</b>	<b>4.8</b>	<b>4.2</b>	<b>4.6</b>	<b>4.3</b>	<b>4.5</b>	<b>1 * A5000 24GB</b>

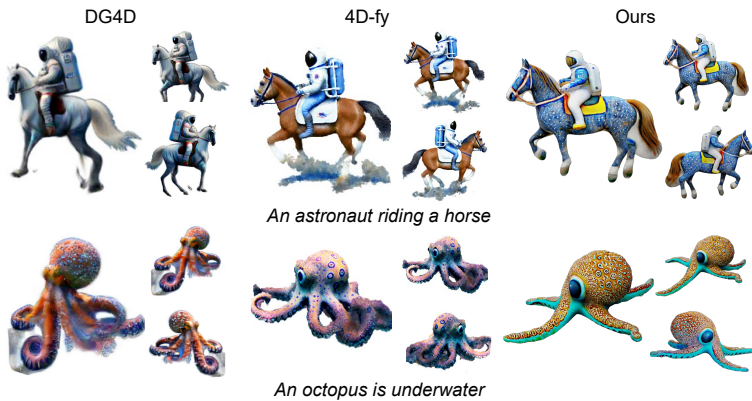


Figure 4. Overall 4D comparison results.

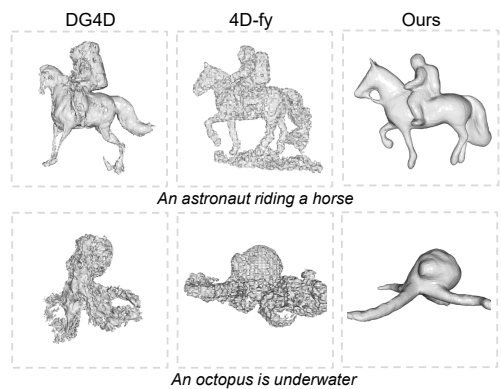


Figure 5. Underlying geometry comparison.

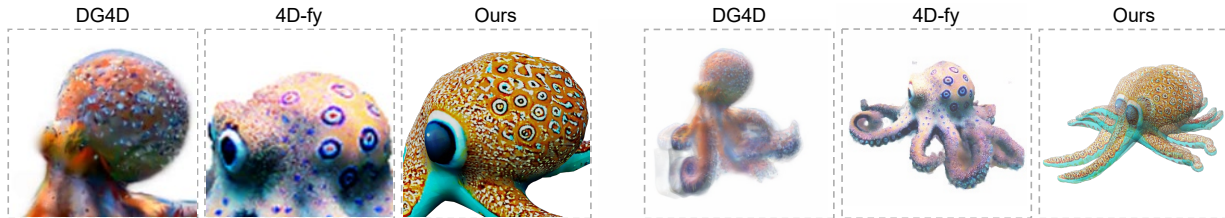


Figure 6. Zoom-in details (left) and motion-centric comparison (right), where opacity conveys motion amplitude: lower opacity indicates larger motion, and vice versa.

where a higher score indicates better alignment with input descriptions. Multiple camera views and frames over time are sampled during the computation of the CLIP score. As shown in Table 1, TextMesh4D achieves the highest mean CLIP score across evaluation prompts among all baselines.

**User study.** We conduct perceptual user studies to evaluate sample quality along the dimensions of *appearance quality (AQ)*, *3D structure quality (SQ)*, *motion quality (MQ)*, *text alignment (TA)*, and *overall preference (Overall)*. A total of 31 participants were recruited for evaluation. Details are provided in the Supplementary Material, and the numerical results are reported in Table 1, which consistently favor our method over the baselines in direct comparisons.

**GPT-4V selection.** Moreover, we follow InterFusion [14]

and further leverage the advanced image understanding capabilities of GPT-4V to enable a more fine-grained evaluation. Specifically, we prompt GPT-4V to select the preferred result based on the same criteria as used in the aforementioned user study. No in-context examples are provided during prompting to maintain a zero-shot setting. Results are reported in Table 1. GPT-4V provides a complementary evaluation to human feedback and further validates the superiority of our method.

#### 4.5. Ablation Study

**Effectiveness of Jacobian Deformation Field (JDF).** We conduct ablation studies to validate the critical role of our proposed JDF in addressing deformation inflexibility. We

compare our full method (Ours) against two ablated variants: 1) Vertex (Var-A), which directly optimizes vertex displacements as in prior works, and 2) Vertex (Var-B), which applies an intermediate rigging structure to vertex displacements for deformation enhancement.

As illustrated in Fig. 7, ablation results (1st and 2nd columns) clearly demonstrate the limitations of vertex-based optimization. The Vertex (Var-A) variant suffers from severe geometric shattering and topological errors, as direct vertex optimization is overly constrained by mesh connectivity, making it incapable of expressing complex deformations. The Vertex (Var-B) variant mitigates the surface-breaking artifacts. However, it exhibits overly rigid dynamics (the unnatural flagpole), and geometric artifacts are still present. In contrast, our JDF method generates a smooth, continuous, and visually plausible deformation. This experiment validates our core insight: by shifting the deformation unit from vertices to faces and modeling transformations via JDF, we effectively release the deformation from rigid topological constraints. This allows our method to achieve both high-fidelity geometric integrity and the expressive flexibility required for complex motions.

**Effectiveness of Local-Global Semantic Regularizer (LGSR)** We also conduct ablation studies to validate our Local-Global Semantic Regularizer (LGSR) in addressing semantic inconsistency, which arises from noisy priors from text-to-video (T2V) models that cause both local surface corruption and global identity drifts. We compare our full method against two ablated variants: 1) w/o G-SR, which applies only the local regularizer, and 2) w/o L-SR, which applies only the global regularizer.

As shown in Fig. 7, ablation results (3rd and 4th columns) demonstrate that both local and global components are indispensable. The w/o L-SR variant highlights the necessity of the local component (L-SR), which provides local rigidity to stabilize local geometry against noisy priors. Without it, the geometry appears stretched like clay during motion (highlighted in red). Conversely, the w/o G-SR variant showcases that the global component (G-SR) is essential for preserving global semantic identity. Without this component, the model fails to preserve the flagpole’s identity (highlighted in red). Our full JDF+LGSR (Ours), leveraging both regularizers, works in tandem to suppress both local and global noise from the T2V prior at the geometric level. This strikes a balance between rigidity and flexibility, and generates natural and high-fidelity results.

## 5. Conclusion

We present TextMesh4D, a novel framework for generating dynamic 3D mesh sequences from text. By shifting the deformation unit from vertices to faces via the Jacobian Deformation Field (JDF), our method overcomes the inherent

Table 2. Quantitative ablation results by GPT-4V.

Settings	GPT-4V Selection (%)				
	AQ	SQ	MQ	TA	Overall
Vertex (Var-A)	1.9	1.0	1.5	1.8	1.1
Vertex (Var-B)	1.1	7.3	0.5	1.3	3.9
w/o G-SR	15.2	9.0	3.4	5.6	7.4
w/o L-SR	5.6	6.9	39.7	26.3	10.3
<b>Ours (JDF+LGSR)</b>	<b>76.2</b>	<b>75.8</b>	<b>55.0</b>	<b>66.0</b>	<b>77.3</b>

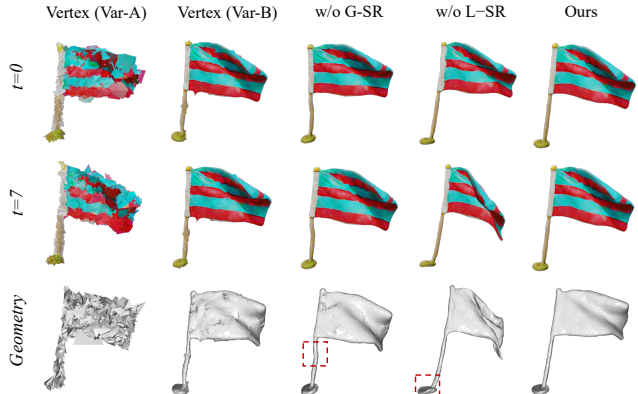


Figure 7. Qualitative ablations with the given text prompt “a flag fluttering in the air”. The top two rows showcase two frames, while the bottom row illustrates the geometry corresponding to the second row.

deformation inflexibility of mesh topology. Furthermore, our proposed Local-Global Semantic Regularizer (LGSR) effectively suppresses stochastic semantic inconsistency introduced by video diffusion priors, ensuring both local motion coherence and global identity consistency. Extensive experiments validate that TextMesh4D sets a new state of the art in temporal stability, geometric fidelity, and visual quality for text-to-4D generation, demonstrating the viability of mesh-centric approaches in 4D content creation.

**Limitations & Future Work.** As our framework follows a two-stage process, where static content is generated first, followed by dynamic motion synthesis, the quality of dynamic generation depends on the success of the static stage. If the static composition is unsatisfactory, it may propagate errors into subsequent motion synthesis, resulting in incorrect accumulations. We believe this issue could be alleviated with further advances in 3D generation techniques.

Furthermore, the optimization space of global transformations is constrained by the camera space of differentiable rendering. Combining our framework with the latest video diffusion models under explicit camera control offers a promising direction. Lastly, given the inherent trade-off between motion stability and diversity, our current design prioritizes generalizability, which limits the ability to handle highly exaggerated motions, such as explosions. Extending TextMesh4D to address such cases will be an interesting avenue for future exploration.

## References

- [1] Zeroscope text-to-video model. [https://huggingface.co/cerspense/zeroscope-v2\\_576w](https://huggingface.co/cerspense/zeroscope-v2_576w), 2023. Accessed: 2023-10-31. 2, 4
- [2] Noam Aigerman, Kunal Gupta, Vladimir G Kim, Siddhartha Chaudhuri, Jun Saito, and Thibault Groueix. Neural jacobian fields: Learning intrinsic mappings of arbitrary meshes. *arXiv preprint arXiv:2205.02904*, 2022. 3
- [3] Sherwin Bahmani, Ivan Skorokhodov, Victor Rong, Gordon Wetzstein, Leonidas Guibas, Peter Wonka, Sergey Tulyakov, Jeong Joon Park, Andrea Tagliasacchi, and David B Lindell. 4d-fy: Text-to-4d generation using hybrid score distillation sampling. In *Proceedings of the IEEE/CVF Conference on Computer Vision and Pattern Recognition*, pages 7996–8006, 2024. 2, 4, 6, 7
- [4] Sherwin Bahmani, Xian Liu, Wang Yifan, Ivan Skorokhodov, Victor Rong, Ziwei Liu, Xihui Liu, Jeong Joon Park, Sergey Tulyakov, Gordon Wetzstein, et al. Tc4d: Trajectory-conditioned text-to-4d generation. In *European Conference on Computer Vision*, pages 53–72. Springer, 2025. 2, 7
- [5] Max Bain, Arsha Nagrani, Gül Varol, and Andrew Zisserman. Frozen in time: A joint video and image encoder for end-to-end retrieval. In *Proc. ICCV*, 2021. 2
- [6] Andreas Blattmann, Tim Dockhorn, Sumith Kulal, Daniel Mendelevitch, Maciej Kilian, Dominik Lorenz, Yam Levi, Zion English, Vikram Voleti, Adam Letts, et al. Stable video diffusion: Scaling latent video diffusion models to large datasets. *arXiv preprint arXiv:2311.15127*, 2023. 1
- [7] Ang Cao and Justin Johnson. Hexplane: A fast representation for dynamic scenes. In *Proceedings of the IEEE/CVF Conference on Computer Vision and Pattern Recognition*, pages 130–141, 2023. 2
- [8] Yukang Cao, Yan-Pei Cao, Kai Han, Ying Shan, and Kwan-Yee K Wong. Dreamavatar: Text-and-shape guided 3d human avatar generation via diffusion models. In *Proceedings of the IEEE/CVF Conference on Computer Vision and Pattern Recognition*, pages 958–968, 2024. 2
- [9] Ce Chen, Shaoli Huang, Xuelin Chen, Guangyi Chen, Xiaoguang Han, Kun Zhang, and Mingming Gong. Ct4d: Consistent text-to-4d generation with animatable meshes. *arXiv preprint arXiv:2408.08342*, 2024. 6
- [10] Haoxin Chen, Menghan Xia, Yingqing He, Yong Zhang, Xiaodong Cun, Shaoshu Yang, Jinbo Xing, Yaofang Liu, Qifeng Chen, Xintao Wang, et al. Videocrafter1: Open diffusion models for high-quality video generation. *arXiv preprint arXiv:2310.19512*, 2023. 2
- [11] Kevin Chen, Christopher B Choy, Manolis Savva, Angel X Chang, Thomas Funkhouser, and Silvio Savarese. Text2shape: Generating shapes from natural language by learning joint embeddings. In *Computer Vision—ACCV 2018: 14th Asian Conference on Computer Vision, Perth, Australia, December 2–6, 2018, Revised Selected Papers, Part III 14*, pages 100–116. Springer, 2019. 2
- [12] Rui Chen, Yongwei Chen, Ningxin Jiao, and Kui Jia. Fantasia3d: Disentangling geometry and appearance for high-quality text-to-3d content creation. In *Proceedings of the IEEE/CVF international conference on computer vision*, pages 22246–22256, 2023. 2
- [13] I2VGen-XL contributors. I2vgen-xl. Accessed October 15, 2023 [Online] <https://modelscope.cn/models/damo/Image-to-Video/summary>, 2023. 2
- [14] Sisi Dai, Wenhao Li, Haowen Sun, Haibin Huang, Chongyang Ma, Hui Huang, Kai Xu, and Ruizhen Hu. Interfusion: Text-driven generation of 3d human-object interaction. *arXiv preprint arXiv:2403.15612*, 2024. 2, 7
- [15] William Gao, Noam Aigerman, Thibault Groueix, Vova Kim, and Rana Hanocka. Textdeformer: Geometry manipulation using text guidance. In *ACM SIGGRAPH 2023 Conference Proceedings*, pages 1–11, 2023. 5
- [16] Xianfan Gu, Chuan Wen, Weirui Ye, Jiaming Song, and Yang Gao. Seer: Language instructed video prediction with latent diffusion models. *arXiv preprint arXiv:2303.14897*, 2023. 2
- [17] Ayaan Haque, Matthew Tancik, Alexei A Efros, Aleksander Holynski, and Angjoo Kanazawa. Instruct-nerf2nerf: Editing 3d scenes with instructions. In *Proceedings of the IEEE/CVF International Conference on Computer Vision*, pages 19740–19750, 2023. 2
- [18] Jonathan Ho, William Chan, Chitwan Saharia, Jay Whang, Ruiqi Gao, Alexey Gritsenko, Diederik P Kingma, Ben Poole, Mohammad Norouzi, David J Fleet, et al. Imagen video: High definition video generation with diffusion models. *arXiv preprint arXiv:2210.02303*, 2022. 1
- [19] Fangzhou Hong, Mingyuan Zhang, Liang Pan, Zhongang Cai, Lei Yang, and Ziwei Liu. Avatarclip: Zero-shot text-driven generation and animation of 3d avatars. *arXiv preprint arXiv:2205.08535*, 2022. 2
- [20] Yukun Huang, Jianan Wang, Yukai Shi, Xianbiao Qi, Zheng-Jun Zha, and Lei Zhang. Dreamtime: An improved optimization strategy for text-to-3d content creation. *arXiv preprint arXiv:2306.12422*, 2023. 2
- [21] Yukun Huang, Jianan Wang, Ailing Zeng, He Cao, Xianbiao Qi, Yukai Shi, Zheng-Jun Zha, and Lei Zhang. Dreamwaltz: Make a scene with complex 3d animatable avatars. *Advances in Neural Information Processing Systems*, 36, 2024. 2
- [22] Takeo Igarashi, Tomer Moscovich, and John F Hughes. As-rigid-as-possible shape manipulation. *ACM transactions on Graphics (TOG)*, 24(3):1134–1141, 2005. 5
- [23] Tansin Jahan, Yanran Guan, and Oliver Van Kaick. Semantics-guided latent space exploration for shape generation. In *Computer Graphics Forum*, pages 115–126. Wiley Online Library, 2021. 2
- [24] Ajay Jain, Ben Mildenhall, Jonathan T Barron, Pieter Abbeel, and Ben Poole. Zero-shot text-guided object generation with dream fields. In *Proceedings of the IEEE/CVF Conference on Computer Vision and Pattern Recognition*, pages 867–876, 2022. 2
- [25] Diederik P Kingma and Jimmy Ba. Adam: A method for stochastic optimization. In *International Conference on Learning Representations*, 2015. 5
- [26] Samuli Laine, Janne Hellsten, Tero Karras, Yeongho Seol, Jaakko Lehtinen, and Timo Aila. Modular primitives for high-performance differentiable rendering. *ACM Transactions on Graphics (ToG)*, 39(6):1–14, 2020. 4

- [27] Han-Hung Lee and Angel X Chang. Understanding pure clip guidance for voxel grid nerf models. *arXiv preprint arXiv:2209.15172*, 2022. 2
- [28] Yuhan Li, Yishun Dou, Yue Shi, Yu Lei, Xuanhong Chen, Yi Zhang, Peng Zhou, and Bingbing Ni. Focaldreamer: Text-driven 3d editing via focal-fusion assembly. In *Proceedings of the AAAI Conference on Artificial Intelligence*, pages 3279–3287, 2024. 2
- [29] Chen-Hsuan Lin, Jun Gao, Luming Tang, Towaki Takikawa, Xiaohui Zeng, Xun Huang, Karsten Kreis, Sanja Fidler, Ming-Yu Liu, and Tsung-Yi Lin. Magic3d: High-resolution text-to-3d content creation. *arXiv preprint arXiv:2211.10440*, 2022. 2
- [30] Huan Ling, Seung Wook Kim, Antonio Torralba, Sanja Fidler, and Karsten Kreis. Align your gaussians: Text-to-4d with dynamic 3d gaussians and composed diffusion models. In *Proceedings of the IEEE/CVF Conference on Computer Vision and Pattern Recognition*, pages 8576–8588, 2024. 2, 7
- [31] Zhengzhe Liu, Yi Wang, Xiaojuan Qi, and Chi-Wing Fu. Towards implicit text-guided 3d shape generation. In *Proceedings of the IEEE/CVF Conference on Computer Vision and Pattern Recognition*, pages 17896–17906, 2022. 2
- [32] William E Lorensen and Harvey E Cline. Marching cubes: A high resolution 3d surface construction algorithm. *ACM siggraph computer graphics*, 21(4):163–169, 1987. 4
- [33] Luke Melas-Kyriazi, Iro Laina, Christian Rupprecht, and Andrea Vedaldi. Realfusion: 360deg reconstruction of any object from a single image. In *Proceedings of the IEEE/CVF conference on computer vision and pattern recognition*, pages 8446–8455, 2023. 2
- [34] Gal Metzer, Elad Richardson, Or Patashnik, Raja Giryes, and Daniel Cohen-Or. Latent-nerf for shape-guided generation of 3d shapes and textures. *arXiv preprint arXiv:2211.07600*, 2022. 2
- [35] Ben Mildenhall, Pratul P Srinivasan, Matthew Tancik, Jonathan T Barron, Ravi Ramamoorthi, and Ren Ng. Nerf: Representing scenes as neural radiance fields for view synthesis. *Communications of the ACM*, 65(1):99–106, 2021. 4
- [36] Nasir Mohammad Khalid, Tianhao Xie, Eugene Belilovsky, and Tiberiu Popa. Clip-mesh: Generating textured meshes from text using pretrained image-text models. In *SIGGRAPH Asia 2022 Conference Papers*, pages 1–8, 2022. 2
- [37] Ryan Po and Gordon Wetzstein. Compositional 3d scene generation using locally conditioned diffusion. In *2024 International Conference on 3D Vision (3DV)*, pages 651–663. IEEE, 2024. 2
- [38] Ben Poole, Ajay Jain, Jonathan T Barron, and Ben Mildenhall. Dreamfusion: Text-to-3d using 2d diffusion. *arXiv preprint arXiv:2209.14988*, 2022. 1, 2
- [39] Guocheng Qian, Jinjie Mai, Abdullah Hamdi, Jian Ren, Aliaksandr Siarohin, Bing Li, Hsin-Ying Lee, Ivan Skokhodov, Peter Wonka, Sergey Tulyakov, et al. Magic123: One image to high-quality 3d object generation using both 2d and 3d diffusion priors. *arXiv preprint arXiv:2306.17843*, 2023. 2
- [40] Alec Radford, Jong Wook Kim, Chris Hallacy, Aditya Ramesh, Gabriel Goh, Sandhini Agarwal, Girish Sastry, Amanda Askell, Pamela Mishkin, Jack Clark, et al. Learning transferable visual models from natural language supervision. In *International conference on machine learning*, pages 8748–8763. PMLR, 2021. 6
- [41] Ohad Rahamim, Ori Malca, Dvir Samuel, and Gal Chechik. Bringing objects to life: 4d generation from 3d objects. *arXiv e-prints*, pages arXiv–2412, 2024. 7
- [42] Aditya Ramesh, Mikhail Pavlov, Gabriel Goh, Scott Gray, Chelsea Voss, Alec Radford, Mark Chen, and Ilya Sutskever. Zero-shot text-to-image generation. In *International conference on machine learning*, pages 8821–8831. Pmlr, 2021. 2
- [43] Jiawei Ren, Liang Pan, Jiaxiang Tang, Chi Zhang, Ang Cao, Gang Zeng, and Ziwei Liu. Dreamgaussian4d: Generative 4d gaussian splatting. *arXiv preprint arXiv:2312.17142*, 2023. 6, 7
- [44] Jiawei Ren, Cheng Xie, Ashkan Mirzaei, Karsten Kreis, Ziwei Liu, Antonio Torralba, Sanja Fidler, Seung Wook Kim, Huan Ling, et al. L4gm: Large 4d gaussian reconstruction model. *Advances in Neural Information Processing Systems*, 37:56828–56858, 2024. 7
- [45] Robin Rombach, Andreas Blattmann, Dominik Lorenz, Patrick Esser, and Bjorn Ommer. High-resolution image synthesis with latent diffusion models. In *Proc. CVPR*, 2022. 1, 2
- [46] Chitwan Saharia, William Chan, Saurabh Saxena, Lala Li, Jay Whang, Emily L Denton, Kamyar Ghasemipour, Raphael Gontijo Lopes, Burcu Karagol Ayan, Tim Salimans, et al. Photorealistic text-to-image diffusion models with deep language understanding. *Advances in neural information processing systems*, 35:36479–36494, 2022. 2
- [47] Christoph Schuhmann, Romain Beaumont, Richard Vencu, Cade Gordon, Ross Wightman, Mehdi Cherti, Theo Coombes, Aarush Katta, Clayton Mullis, Mitchell Wortsman, et al. Laion-5b: An open large-scale dataset for training next generation image-text models. *Proc. NeurIPS*, 2022. 2
- [48] Etai Sella, Gal Fiebelman, Peter Hedman, and Hadar Averbuch-Elor. Vox-e: Text-guided voxel editing of 3d objects. In *Proceedings of the IEEE/CVF International Conference on Computer Vision*, pages 430–440, 2023. 2
- [49] Yichun Shi, Peng Wang, Jianglong Ye, Mai Long, Kejie Li, and Xiao Yang. Mvdream: Multi-view diffusion for 3d generation. *arXiv preprint arXiv:2308.16512*, 2023. 2, 4
- [50] Uriel Singer, Adam Polyak, Thomas Hayes, Xi Yin, Jie An, Songyang Zhang, Qiyuan Hu, Harry Yang, Oron Ashual, Oran Gafni, et al. Make-a-video: Text-to-video generation without text-video data. *arXiv preprint arXiv:2209.14792*, 2022. 1
- [51] Uriel Singer, Shelly Sheynin, Adam Polyak, Oron Ashual, Iurii Makarov, Filippos Kokkinos, Naman Goyal, Andrea Vedaldi, Devi Parikh, Justin Johnson, et al. Text-to-4d dynamic scene generation. *arXiv preprint arXiv:2301.11280*, 2023. 2
- [52] Jascha Sohl-Dickstein, Eric Weiss, Niru Maheswaranathan, and Surya Ganguli. Deep unsupervised learning using nonequilibrium thermodynamics. In *International confer-*

- ence on machine learning, pages 2256–2265. PMLR, 2015. 1
- [53] Chaoyue Song, Xiu Li, Fan Yang, Zhongcong Xu, Jiacheng Wei, Fayao Liu, Jiashi Feng, Guosheng Lin, and Jianfeng Zhang. Puppeteer: Rig and animate your 3d models. *arXiv preprint arXiv:2508.10898*, 2025. 7
- [54] Jiaming Song, Chenlin Meng, and Stefano Ermon. Denoising diffusion implicit models. *arXiv preprint arXiv:2010.02502*, 2020. 1
- [55] Jiayang Tang, Jiawei Ren, Hang Zhou, Ziwei Liu, and Gang Zeng. Dreamgaussian: Generative gaussian splatting for efficient 3d content creation. *arXiv preprint arXiv:2309.16653*, 2023. 2
- [56] Junshu Tang, Tengfei Wang, Bo Zhang, Ting Zhang, Ran Yi, Lizhuang Ma, and Dong Chen. Make-it-3d: High-fidelity 3d creation from a single image with diffusion prior. In *Proceedings of the IEEE/CVF international conference on computer vision*, pages 22819–22829, 2023. 2
- [57] Christina Tsalicoglou, Fabian Manhardt, Alessio Tonioni, Michael Niemeyer, and Federico Tombari. Textmesh: Generation of realistic 3d meshes from text prompts. In *2024 International Conference on 3D Vision (3DV)*, pages 1554–1563. IEEE, 2024. 2
- [58] Haochen Wang, Xiaodan Du, Jiahao Li, Raymond A Yeh, and Greg Shakhnarovich. Score jacobian chaining: Lifting pretrained 2d diffusion models for 3d generation. In *Proceedings of the IEEE/CVF Conference on Computer Vision and Pattern Recognition*, pages 12619–12629, 2023. 2
- [59] Jiuniu Wang, Hangjie Yuan, Dayou Chen, Yingya Zhang, Xiang Wang, and Shiwei Zhang. Modelscope text-to-video technical report. *arXiv preprint arXiv:2308.06571*, 2023. 1, 2
- [60] Peng Wang, Lingjie Liu, Yuan Liu, Christian Theobalt, Taku Komura, and Wenping Wang. Neus: Learning neural implicit surfaces by volume rendering for multi-view reconstruction. *arXiv preprint arXiv:2106.10689*, 2021. 4
- [61] Wenjing Wang, Huan Yang, Zixi Tuo, Huiguo He, Junchen Zhu, Jianlong Fu, and Jiaying Liu. Videofactory: Swap attention in spatiotemporal diffusions for text-to-video generation. *arXiv preprint arXiv:2305.10874*, 2023. 2
- [62] Xiang Wang, Hangjie Yuan, Shiwei Zhang, Dayou Chen, Jiuniu Wang, Yingya Zhang, Yujun Shen, Deli Zhao, and Jingren Zhou. Videocomposer: Compositional video synthesis with motion controllability. *arXiv preprint arXiv:2306.02018*, 2023. 2
- [63] Zhengyi Wang, Cheng Lu, Yikai Wang, Fan Bao, Chongxuan Li, Hang Su, and Jun Zhu. Prolificdreamer: High-fidelity and diverse text-to-3d generation with variational score distillation. *Advances in Neural Information Processing Systems*, 36, 2024. 2
- [64] Jinbo Xing, Menghan Xia, Yong Zhang, Haoxin Chen, Wangbo Yu, Hanyuan Liu, Gongye Liu, Xintao Wang, Ying Shan, and Tien-Tsin Wong. Dynamicrafter: Animating open-domain images with video diffusion priors. In *European Conference on Computer Vision*, pages 399–417. Springer, 2025. 2
- [65] Dejia Xu, Hanwen Liang, Neel P Bhatt, Hezhen Hu, Hanxue Liang, Konstantinos N Plataniotis, and Zhangyang Wang. Comp4d: Llm-guided compositional 4d scene generation. *arXiv preprint arXiv:2403.16993*, 2024. 2
- [66] Jiale Xu, Xintao Wang, Weihao Cheng, Yan-Pei Cao, Ying Shan, Xiaohu Qie, and Shenghua Gao. Dream3d: Zero-shot text-to-3d synthesis using 3d shape prior and text-to-image diffusion models. In *Proceedings of the IEEE/CVF Conference on Computer Vision and Pattern Recognition*, pages 20908–20918, 2023. 2
- [67] Yifei Zeng, Yanqin Jiang, Siyu Zhu, Yuanxun Lu, Youtian Lin, Hao Zhu, Weiming Hu, Xun Cao, and Yao Yao. Stag4d: Spatial-temporal anchored generative 4d gaussians. *arXiv preprint arXiv:2403.14939*, 2024. 7
- [68] Yufeng Zheng, Xueting Li, Koki Nagano, Sifei Liu, Otmar Hilliges, and Shalini De Mello. A unified approach for text- and image-guided 4d scene generation. In *Proceedings of the IEEE/CVF Conference on Computer Vision and Pattern Recognition*, pages 7300–7309, 2024. 4, 7
- [69] Jingyu Zhuang, Chen Wang, Liang Lin, Lingjie Liu, and Guanbin Li. Dreameditor: Text-driven 3d scene editing with neural fields. In *SIGGRAPH Asia 2023 Conference Papers*, pages 1–10, 2023. 2